Distinct Families of Z-line Targeting Modules in the COOH-terminal Region of Nebulin

K. Ojima,* Z.X. Lin,§ M.-L. Bang,‖ S. Holtzer,* R. Matsuda,¶ S. Labeit, H.L. Sweeney,‡ and H. Holtzer***

*Department of Cell and Developmental Biology, ‡Department of Physiology, The School of Medicine, University of Pennsylvania, Philadelphia, Pennsylvania 19104; §Department of Cell Biology, Beijing Institute for Cancer Research, Beijing Medical University, Beijing 100034, China; ‖EMBL, Heidelberg, Germany 69012; ¶Department of Life Science, University of Tokyo, Tokyo, Japan 153-8092; and **Department of Anesthesiology and Intensive Operative Care, Klinikum, Mannheim, Germany

Abstract. To learn how nebulin functions in the assembly and maintenance of I-Z-I bands, MYC- and GFP-tagged nebulin fragments were expressed in primary cultured skeletal myotubes. Their sites of incorporation were visualized by double staining with anti-MYC, antibodies to myofibrillar proteins, and FITC- or rhodamine phalloidin. Contrary to expectations based on in vitro binding studies, none of the nebulin fragments expressed in maturing myotubes were incorporated selectively into I-band ~1.0-μm F-α-actin–containing thin filaments. Four of the MYC/COOH-terminal nebulin fragments were incorporated exclusively into periodic ~0.1-μm Z-bands. Whereas both anti-MYC and Rho-phalloidin stained intra-Z-band F-α-actin oligomers, only the latter stained the pointed ends of the polarized ~1.0-μm thin filaments. Z-band incorporation was independent of the nebulin COOH-terminal Ser or SH3 domains. In vitro cosedimentation studies also demonstrated that nebulin SH3 fragments did not bind to F-α-actin or α-actinin. The remaining six fragments were not incorporated into Z-bands, but were incorporated (a) diffusely throughout the sarcoplasm and into (b) fibrils/patches of varying lengths and widths nested among normal striated myofibrils. Over time, presumably in response to the mediation of muscle-specific homeostatic controls, many of the ectopic MYC-positive structures were resorbed. None of the tagged nebulin fragments behaved as dominant negatives; they neither blocked the assembly nor induced the disassembly of mature striated myofibrils. Moreover, they were not cytotoxic in myotubes, as they were in the fibroblasts and presumptive myoblasts in the same cultures.

Key words: Z-bands • myogenesis • I-Z-I bands • α-actin • phalloidin staining

Introduction

Given the conservation, complexity and densely packed configuration of Z-discs (Morris et al., 1990; Goldstein et al., 1991; Vigoreaux, 1994; Schroeter et al., 1996; Gregorio et al., 1999), it might be expected that the expression of mutants and/or fragments of I-Z-I proteins, which lacked appropriate binding sites, would not be incorporated into their normal location in maturing striated myofibrils (SMFs), but would behave as dominant negatives, interfering with the assembly of normal sarcomeres and probably be cytotoxic. However, we reported that expression of 14/16 MYC/sarcomeric α-actinin (s-α-actinin)[1] peptides that lacked their actin and/or titin binding sites, as well as those lacking their four spectrin repeats or calmodulin binding sites, was promptly incorporated exclusively into normal precursor and mature Z-discs when expressed in transfected maturing myotubes (Schultheiss et al., 1992; Holtzer et al., 1997; Lin et al., 1998; Ojima et al., 1999). Despite binding/bundling filamentous actin (F-actin) in cell-free systems, MYC/s-α-actinin did not bind to the polarized ~1.0-μm long F-α-actin–containing thin filaments in differentiating myotubes. It was suggested that, in maturing myotubes, the binding between s-α-actinin and F-α-actin along the ~1.0-μm thin filaments might be blocked by tropomyosin and/or troponin complexes, whereas the s-α-actinin binding sites along the actin oligomers within the Z-band (Yamaguchi et al., 1985) remained available for the incorporation of the MYC/s-α-actinin mutants. Unexpectedly, these truncated MYC/s-α-actinin peptides did not assemble into ectopic structures, behave as dominant negatives, nor were they obviously cytotoxic.

Address correspondence to Howard Holtzer, Department of Cell and Developmental Biology, 1051 BRB II/III, The School of Medicine, University of Pennsylvania, 421 Curie Boulevard, Philadelphia, PA 19104. Tel.: (215) 898-8089. Fax: (215) 898-9871. E-mail: hholtzer@mail.med.upenn.edu

[1]*Abbreviations used in this paper:* DAPI, 4, 6-diamidino-2-phenylindole dihydrochloride; F-actin, filamentous actin; MHC, myosin heavy chain; Rho-phalloidin, rhodamine phalloidin; s-α-actinin, sarcomeric α-actinin; SMF, striated myofibril.

Of the 16 mutants, only the MYC/s-α-actinin lacking the EF-hands and titin binding domain induced hypertrophied Z-bands, or nemaline-like bodies. In brief, MYC/s-α-actinin fragments that would have been predicted to be assembly-incompetent on the basis of in vitro binding studies were, in fact, incorporated into normal precursor I-Z-I bodies and mature Z-band structures when expressed in maturing myotubes. Such apparent discrepancies between in vitro and in vivo binding prompted us to determine whether they reflected unique properties of the following: (1) s-α-actinin as a multifunctional ligand; (2) the presence of available and unsaturated receptors in maturing intra-Z-band structures; or (3) cell type–specific homeostatic controls, which enable maturing myotubes to cope with malformed MYC/s-α-actinin molecules and/or structures (e.g., differential turnover, posttranslational changes of improperly configured peptides, etc.). Accordingly, the same experimental protocols used with MYC/s-α-actinin fragments have now been used to follow the temporospatial incorporation of MYC/COOH-terminal nebulin fragments into I-Z-I bands in maturing day 4–10 myotubes.

Nebulin, a giant actin binding protein (~800 kD), is a component of vertebrate skeletal sarcomeres (Wang and Williamson, 1980; Wang and Wright, 1988; Kruger et al., 1991; Labeit et al., 1991; Wright et al., 1993; Labeit and Kolmerer, 1995). In situ, a single molecule is incorporated into, and is coextensive in length with, ~1.0-μm polarized I-band thin filaments (Wang and Wright, 1988; Wright et al., 1993). Its NH_2 terminus extends to the pointed end of the F-α-actin thin filament complex, whereas its COOH terminus is an intra-Z-disc component. On the sequence level, nebulin consists of ~185 modules, depending on the respective isoform (Labeit and Kolmerer, 1995). Each module is made up of ~35 amino acid residues, which contain a central SDXXYK consensus motif. The central 154 modules are organized into 22 super-repeats. Each super-repeat consists of seven modules, which are thought to reflect the periodicity of the ~1.0-μm F-α-actin thin filament complex. Recombinant nebulin, containing 2–15 modules, as well as single synthetic nebulin modules, display a strong affinity to F-actin in in vitro binding assays, but truncated modules do not (Root and Wang, 1994; Pfuhl et al., 1994, 1996; Gonsior et al., 1998; Zhang et al., 1998). Nebulin's COOH terminus appears to be located 25–30 nm inside the Z-line (Millevoi et al., 1998). This part of nebulin involves COOH-terminal modules M177-M185, plus a Ser-rich region containing multiple phosphorylation sites, and a COOH-terminal SH3 domain. How this COOH-terminal region of ~400 amino acids might interact with such intra Z-disc peptides as F-α-actin, s-α-actinin, T-cap, or the NH_2-terminal ~900 amino acids of titin is unclear (Wang et al., 1996; Maruyama, 1997; Mues et al., 1998; Politou et al., 1998; Gautel et al., 1999; Gregorio et al., 1999). The activity of Ser and SH3 domains in the assembly and disassembly of cytoskeletal structures has invited speculations that they might be involved in the assembly of Z-bands during myofibrillogenesis.

Experiments were designed to determine which nebulin modules, when expressed in transfected skeletal myogenic cells, might do the following: (1) be incorporated exclusively into Z-discs; (2) bind continuously along the polarized ~1.0-μm F-α-actin–containing thin filaments; (3) assemble into ectopic structures; (4) interfere as dominant negatives with either the assembly or maintenance of normal I-Z-I structures; or (5) be cytotoxic. Moreover, by following the changing distribution of exogenous MYC/nebulin modules over time, we could also determine whether day 10 myotubes could cope with aberrant nebulin peptides more efficiently than day 4 myotubes.

Materials and Methods

Cell Culture and Transfection Procedures

Primary cultures of myogenic cells were obtained from a day 11 chick embryonic pectoral muscle (Antin et al., 1986). Trypsinized cells were plated onto collagen-coated Aclar coverslips (Pro-Plastics) at an initial density of 4.5×10^5 cells per 35-mm culture dish. 24-h cultures were transfected with various MYC/nebulin or GFP/nebulin constructs, using a calcium phosphate precipitation method (Lin et al., 1998; Ojima et al., 1999). Transfection reagents were purchased from Eppendorf-5Prime, Inc. (80303).

Constructs Preparations

pcDNA3-myc Nebulin. All nebulin constructs were obtained from a human leg muscle cDNA library (CLONTECH Laboratories Inc.). 10–30 ng of total cDNA was amplified by 25 cycles of PCR amplification, using 10 s 95°C for denaturation, and 6 min 68°C for combined primer annealing/fragment extension. Primer sequences were derived from nebulin's human cDNA sequence (EMBL data library X83957), and located at module boundaries as inferred from sequence alignments of M1-M185 (Pfuhl et al., 1996); M175S, 5′-tttgaattct ACACCTGAGATGATGAGAGTGAAACAAACA-3′; M185S, 5′-tttgaattct GAACAAAAACGGAATGACCAAGATCAG-3′; SH3R, 5′-tttctcg AGGATCTGTAAGTCCTGCAGACAAGTGTGA-3′; SerR, 5′-tttctcgagcta AGATGGATGAGATGGGATGGAAGATACCGT-3′; M184R, tttctcgagcta CATTTCTACCACTTTCCTCTGAATACCTCG-3′; SR12R1aS, 5′-tttgaattct GCCCGGAACATTGAAGATGACCCCAAGATGATG-3′; SR12R7aR, 5′-tttctcgagcta TCGGGCGCCAATGTGGTGACCCAACTGCTT-3′; M160S, 5′-cggaattcc CTCAGATCCTGCTGGCG-3′; M171S, 5′-cggaattcc CCGGATTTTATGAGGGCC-3′; M175R, 5′-ccgctcgagcta CAGGTCAGGGATTGG-3′; and M183R, 5′-ccgctcgagcta ATCTGTCACCACTGG-3′. M86–M92, the 12th super-repeat region of nebulin, contained the fragments of SR12R1aS-SR12R7aR. M160-M183, COOH-terminal nebulin 24 modules without Ser-rich and SH3 domains, contained the fragments of M160S-M183R. M160-M175, just outside of the Z-bands, contained the fragments of M160S-M175R. M171-M183, outside and inside area of the Z-band nebulin modules, contained M171S-M183R fragments. M175-M184, the borderline of Z-bands, contained the fragments of M175S-M184R. M175-SH3, nebulin COOH-terminal 11 modules and Ser-rich domain plus SH3 domain, contained the PCR products of M175S-SH3R. M175-Ser, nebulin COOH-terminal region without SH3 domain, contained M175S-SerR fragments. M185-SH3, one module and serine-rich domain plus SH3 domain, contained M185S-SH3R products. M185-Ser, one module and serine-rich domain, contained the fragments of M185S-SerR. After all PCR products were digested with EcoRI and XhoI, they were subcloned into the myc-tagged pcDNA3 vector (Invitrogen; Ojima et al., 1999).

pEGFP-C1-nebulin. Nebulin M86-M92 fragments, the 12th super-repeat region of nebulin, were amplified with a pair of sense and antisense primers; SR12R1S, 5′-tttagatct GCCCGGAACATTGAAGATGACCCCAAGATGATG-3′; SR12R7R, 5′-tttgtcgacta TCGGGCGCCAATGTGGTGACCCAACTGCTT-3′. Generated DNA products were digested with BglII and AccI, and introduced into pEGFP-C1 vector (CLONTECH Laboratories, Inc.). All plasmids were purified with QIAGEN column, and all constructs were confirmed by sequencing. See Fig. 1 for a summary of the 10 tagged constructs and their approximate spatial relationship to the I-Z-I bands in a relaxed sarcomere.

Antibodies

To detect the expressed MYC-tagged peptides, monoclonal anti-myc antibody (1:10) or rabbit polyclonal anti-myc antibody (1:200; Upstate Biotechnology) was used. Monoclonal anti-myc antibodies were produced from the hybridoma MYC 9E10. Antibodies specific to various sarcomeric proteins were used. S-α-actinin was localized with an mAb, 9A2B8 (1:400;

Lin et al., 1998). mAbs against cardiac α-actin (1:10; clone Acl-20-4.2) and against skeletal α-actin (1:400; clone 5C5) were purchased from American Research Products and Sigma Chemical Co., respectively. They do not stain actin isoforms in nonmuscle cells (Lin et al., 1987; Franke et al., 1996). Intra-Z-band titin epitopes were localized with polyclonal antititin Z1-Z2 (1:50; Gregorio et al., 1998). To visualize endogenous nebulin, monoclonal antinebulin (1:50; NB2) was purchased from Sigma Chemical Co. To visualize intra-Z-band nebulin, anti-SH3 antibody was used (1:10; Millevoi et al., 1998). Myosin heavy chains (MHCs) were followed with an mAb (F59; 1:20; Miller et al., 1989) and a polyclonal (Organon Teknika Corp.). An affinity-purified rabbit antitropomyosin (1:400) was purchased from Organon Teknika Corp.; its specificity for I-band filaments was demonstrated in Ojima et al. (1999).

Microscopy

Indirect immunofluorescence double staining has been detailed by Lin et al. (1998) and Ojima et al. (1999). In brief, day 3–10 cultures were fixed with 2% formaldehyde in PBS for 3 min after washing with PBS. Cultures were permeabilized with 0.5% Triton X-100 in PBS and treated with blocking buffer (BB; 2% BSA in PBS) for 30 min to minimize nonspecific binding. Samples were incubated with primary antibody for 1 h at 37°C. After washing with 0.5% Triton X-100 in PBS, specimens were reacted with secondary antibody for 1 h at 37°C. Affinity-purified secondary antibodies (Jackson ImmunoResearch Laboratories) were conjugated with rhodamine, Texas red or FITC. To localize F-actin, some dishes were stained with Rho-, Texas red–, or FITC-phalloidin (3.3 μM; Molecular Probes, Inc.). In some series, the cells were exposed to either phalloidin for 10 min, in others for 30 or 60 min. As a control for artifactual bleedthrough, all double-stained preparations were run in duplicate. In one series, each of the two primary antibodies was stained with either a rhodamine- or a fluorescein-conjugated secondary antibody. In the second series, the same primary antibodies were stained in the opposite fashion; thus, each antigen was localized by the use of both fluorescein- and rhodamine-tagged secondary antibodies. Nuclei were detected with 4, 6-diamidino-2-phenylindole dihydrochloride (DAPI; Polyscience). Specimens were mounted in 60% glycerol in PBS containing 2.5% DABCO (1, 4-diazabicyclo (2,2,2) octane; Sigma Chemical Co.). Micrographs were recorded on 400 ASA film (T-MAX; Eastman Kodak Co.). All images were analyzed with Adobe Photoshop (version 5.02).

Single- and double-stained cells were also observed using a laser scanning confocal microscope (LSM 510; Carl Zeiss, Inc.), which employed a Zeiss Axiovert inverted microscope. Images were viewed with a Zeiss C-Apo 63× water immersion objective lens (NA 1.2). The 488- and 568-nm lines were excited by an argon-krypton laser. Rhodamine and fluorescein signals were visualized using appropriate filters. Images were taken in the z-axis of ~1-μm optical sections. The staining intensity profiles illustrated in Fig. 4 (B and D) were based on LSM510 imaging software (version 2.3).

Z-bands, which measure ~0.1 μm in width in EM sections, appear to measure ~0.25 μm in the fluorescence microscope after staining with antibodies to s-α-actinin or antinebulin (Lin et al., 1998; see Fig. 4). Given the limited resolution of the fluorescence microscope and to avoid confusion in the text, the size of fluorescent Z-bands was taken as ~0.1 μm. The slight errors in estimating size resulting from this procedure did not alter our interpretation of the data. Conventional EM sections were prepared and examined in a Type H-800 (Hitachi Ltd.) as described in Toyama et al. (1982) and Lin et al. (1998).

Purification of the Nebulin SH3 Domain

The cDNA coding for the human nebulin SH3 domain (residues 6,610–6,669, EMBL data library No. AC X83957) was cloned into a His-tagged pET vector (Studier et al., 1990). Transformed BL2l (DE3) cells were inoculated into prewarmed (37°C) LB medium containing 50 μg/ml kanamycin. At the end of their logarithmic phase, the cells were induced with 0.2 mM isopropyl-β-D-thiogalactopyranoside overnight at 200 rpm at 18°C. The cell pellets were harvested and frozen. The frozen cells were thawed in a lysis buffer (200 mM NaCl, 20 mM Tris-HCl, pH 8.0), 10 mM imidazole, 2 mM β-mercaptoethanol 0.2% (vol/vol), Igepal CA-630 (Sigma Chemical Co.) containing 200 μg/ml lysozyme, and subsequently sonicated. The soluble overexpressed protein was purified by nickel-NTA agarose (QIAGEN) chromatography and eluted with 200 mM imidazole, pH 8.0. The SH3-containing fractions were dialyzed against 20 mM Tris-HCl, pH 8.0, 2 mM EDTA, 1 mM DTT, and further purified by chromatography on a Q-Sepharose resign (Pharmacia Biotech). The nebulin SH3 domain eluted at ~250 mM NaCl, and fractions containing the protein were concentrated in a Centriplus concentrator (Amicon) by centrifugation. The purity of the protein was confirmed by SDS-PAGE, and was seen as a protein of ~8 kD.

Sedimentation Assay

In vitro cosedimentation assays were performed as described by van Straaten et al. (1998). The protein concentrations used were in all cases 0.29 mg/ml (38.3 μM) of purified SH3 domain, 0.12 mg/ml (2.8 μM) of F-actin from rabbit skeletal muscle (prepared as described in Bullard et al., 1985) and 0.37 mg/ml (3.7 μM) of α-actinin from rabbit skeletal muscle (prepared by the method of Langer and Pepe, 1980). The proteins were mixed in F-buffer (0.1 M NaCl, 10 mM Tris, pH 7.5, l mM $MgCl_2$, 1 mM NaN_2) to a total volume of 106 μl. The samples were placed at room temperature for 30 min, and subsequently centrifuged for 30 min in a Beckman airfuge. The pellets were taken up in 30 μl of water, and the supernatants were reduced to a volume of 55 μl in a speedvac. One sixth the volumes of pellets and supernatants were loaded on a 4–20% SDS-PAGE gradient gel (Bio-Rad Laboratories). Proteins were visualized by Coomassie blue staining.

Results

Localization of MYC/M160-M183 and M160-M175

The shafts of >90% of day 4–10 (Fig. 2, A and A′) myotubes are rich in newly assembled mature striated myofibrils (SMFs). Each I-band consists of ~1.0-μm F-α-actin/tropomyosin/troponin complexes that insert into periodic Z-bands by their barbed ends (Ishikawa et al., 1969). Each ~0.1-μm wide Z-band has been claimed to be positive for s-α-actinin, F-α-actin, titin, nebulin, and T-cap (Lin et al., 1998; Ojima et al., 1999).

Expressed MYC/M160-M183 and MYC/M160-M175 (Fig. 1) were incorporated exclusively into periodic ~0.1-μm

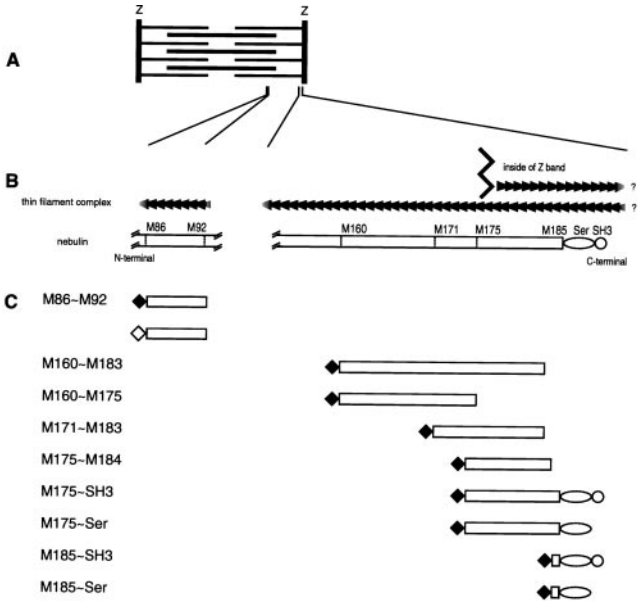

Figure 1. Schematic representations of (A) a single sarcomere; (B) relationships of the polarized F-α-actin filaments from adjacent sarcomeres, in and outside of, the Z-band relative to the COOH-terminal of nebulin (Gregorio et al., 1999); and (C) MYC- (◆) and GFP (◇)-tagged nebulin constructs used in this report. The intra-Z-band region of nebulin contains nine modules (M177-M185), plus a Ser-rich, and an SH3 domain. Little is known of the interrelationships of nebulin with other Z-band proteins, which include F-α-actin oligomers, s-α-actinin, T-Cap, as well as the COOH-terminal titin ~900 amino acid residues.

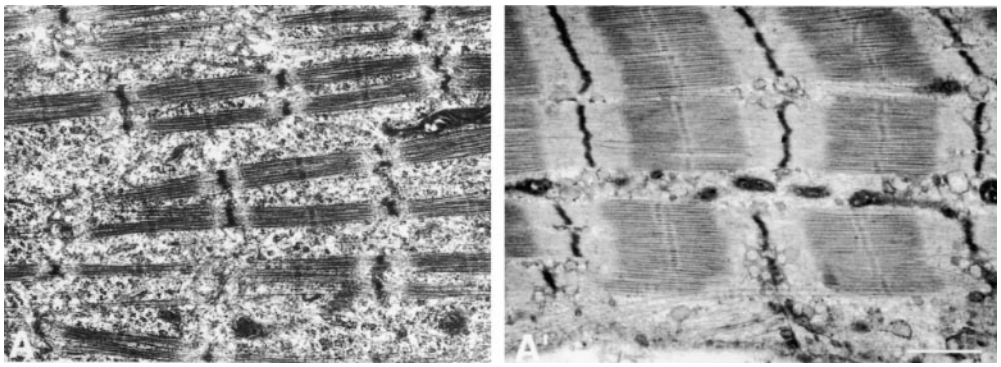

Figure 2. EM sections documenting the advanced stages of differentiation achieved by nascent SMFs in control cultured chick myotubes. Fig. 2 A is of a day 4 myotube, and Fig. 2 A′ is of a day 10 myotube. In ultrastructural details, day 10 SMFs are virtually indistinguishable from those in newly hatched chickens (Takekura et al., 1993). This advanced degree of maturation of SMFs, SR, T-system, etc., has not been described in cultured myotubes prepared from immortalized myogenic cell lines and is pertinent to the findings in this report (see below). Bar, 1 μm.

wide Z-discs in day 4, 6, and 10 myotubes. Double staining with anti-MYC and antibodies to endogenous s-α-actinin (Fig. 3, A and A′ and B and B′) revealed precise costaining of all MYC/Z-discs. These MYC/nebulin peptides did not do the following: (1) bind to the ~1.0-μm F-α-actin–containing I-band filaments; (2) accumulate diffusely in the sarcoplasm; (3) assemble ectopic longitudinal fibrils/patches (see below); or (4) behave as dominant negatives by perturbing the morphology of the nascent MYC/Z-discs. Double staining with anti-MYC and antibodies to MHC (Fig. 3, C–C′′), titin Z1Z2, or tropomyosin (data not shown) also revealed normal SMFs in these transfected myotubes.

To further delineate the spatial relationships between the incorporation of these MYC/modules and their failure to bind along the ~1.0-μm polarized thin filaments two double staining experiments were performed. Day 10 MYC/M160-M183–transfected cultures were stained with anti-MYC and mAbs to either cardiac- or skeletal α-actin (anti–c- or anti–s-α-actin), or (b) anti-MYC and Rho-phalloidin. For reasons not yet understood, the mAbs to both F-α-actins do not localize within the Z-bands proper, either in normal developing (Lin et al., 1987, 1998) or adult (Otey et al., 1988) SMFs. Rather, in both developing and adult SMFs, the anti–α-actins continuously decorate regions of the polarized I-band filaments up to, but not including, the Z-bands. Similarly, in double-stained MYC/M160-M183–transfected myotubes, while the α-antiactins localize along part of the ~1.0-μm I-band complexes, they are excluded from the Z-band proper (Fig. 3, D–D′′; see similar pattern in SMFs in cultured cardiomyocytes in Handel et al., 1991). Failure of the mAbs to α-actin to decorate the entire thin filament, particularly the intra-Z-band, F-α-actin is not likely due to steric hindrance owing to the size of the IgG molecules. For antibodies to s-α-actinin, nebulin (SH3), and titin (Z1Z2) double stain intra-Z-band components. It will be important to understand why the anti–α-actins fail to bind to the intra-Z-band F-α-actin oligomers (Yamaguchi et al., 1985), but bind those elsewhere in the thin filament complexes (Lin et al., 1998).

While FITC- and Rho-phalloidin are invaluable for detecting F-actin in cell-free systems and in a variety of cytoskeletal structures in nonmuscle cells, their binding to F-α-actin in ~1.0-μm thin filament complexes is not well understood. Under a variety of conditions (e.g., tension, rigor, presence of nebulin, sarcomere length, time in stain, concentration, etc.), neither phalloidin stains the ~1.0-μm I-band filaments uniformly. Rather, they bind to multiple bands per sarcomere (Bukatina et al., 1984; Antin et al., 1986; Wilson et al., 1986; Ao and Lehrer, 1995; Yasuda et al., 1995; Zhukarev et al., 1997). As illustrated in Figs. 3 (E–E′′) and 4 (A–D), while anti–s-α-actinin and anti-MYC localized uniquely in Z-discs, FITC- or Rho-phalloidin stains three separate bands/sarcomere. One band coincides with the narrow Z-discs, the other broader bands are limited to the distal ends of the thin filaments. Whereas the phalloidins bind to the intra-Z-band F-actin oligomers, others that stretch along the length of the ~1.0-μm thin filament are either relatively inaccessible, differentially quenched or enhanced, or have a higher off-rate to the F-actin staining reagents (see Materials and Methods and Discussion). Whether the discontinuity of phalloidin staining at sites along the length of I-band thin filaments is due to local structural inhomogeneites, or local reconfigurations in F-α-actin induced by other myofibrillar molecules (e.g., Ao and Lehrer, 1995; Nagaoka et al., 1995; McGough et al., 1997), has yet to be determined.

In summary, in contrast to data on the actin-binding properties of nebulin modules (regions M9–M179; Wang et al., 1996; Gonsior et al., 1998; Zhang et al., 1998) which bind and polymerize F-actin filaments in vitro, binding of MYC/M160-M183 or MYC/M160-M175 to polarized F-α-actin I-band filaments was not observed in developing myotubes. Both nebulin fragments were incorporated exclusively into periodic 0.1-μm Z-bands. If they behaved as dominant negatives or were cytotoxic (see below), then these effects could not be detected microscopically. It is worth noting that similar findings were reported for most of the MYC/s-α-actinin fragments, the other major intra-Z-band actin-binding protein (Schultheiss et al., 1992; Lin et al., 1998; Ojima et al., 1999).

Localization of MYC/M171-M183

The temporospatial incorporation of MYC/M171-M183 (Fig. 1) differed from that of MYC/M160-M183 and MYC/M160-M175. Equally important, the fate of this particular MYC/nebulin peptide differed in day 4–6 versus day 10

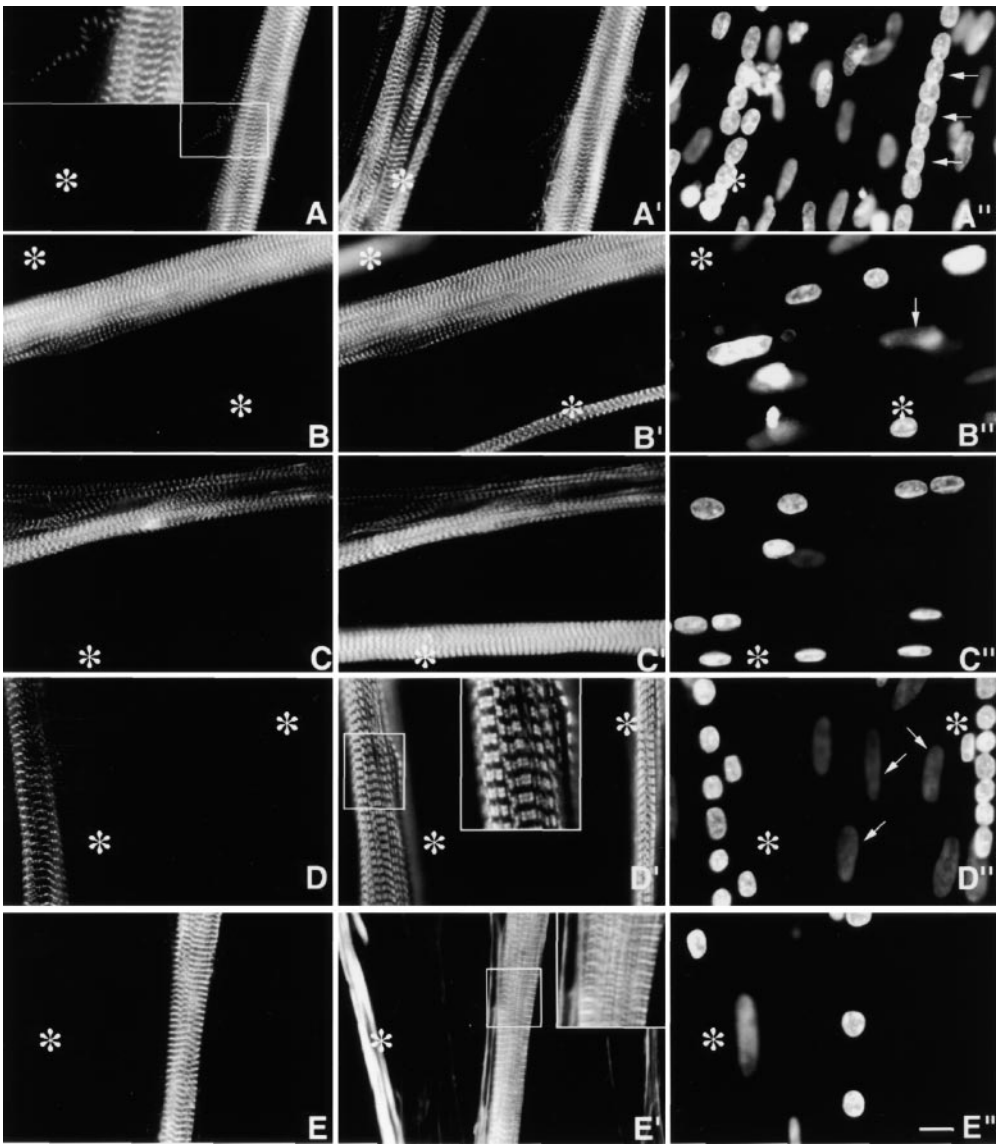

Figure 3. Day 4 MYC/M160-M183 transfected culture triple stained with (A) anti-MYC, (A′) anti-s-α-actinin, and (A′′) DAPI. Asterisks mark a cluster of untransfected myotubes. Note the precise costaining and restricted localization of the two antibodies to morphologically normal Z-bands. They do not stain any region along the ~1.0-μm thin filament complexes. The exogenous peptides do not act as dominant negatives, nor are they cytotoxic. Inset is a higher magnification of a single thin detached SMF. Note the morphological maturity of the Z-bands in this fine SMF. Arrows in A′′ point to aligned nuclei in transfected myotube. (B–B′′) Day 10 MYC/M160-M183–transfected myotube triple stained as in A–A′′. Again, note the precise colocalization and high signal to noise ratio of the anti-MYC and the anti-s-α-actinin. Out-of-focus mononucleated cells indicated by arrows. (C–C′′) Day 4 MYC/M160-M175–transfected culture, triple stained with (C) anti-MYC, (C′) anti-MHC, and (C′′) DAPI. In C′, note the normal ~l.6-μm wide A-bands in both the untransfected (asterisks) and transfected myotube. Day 10 MYC/M160-M183–transfected culture, triple stained with (D) anti-MYC, (D′) anti–c-α-actin and (D′′) DAPI. While the anti-MYC localizes to the Z-bands, the anti–c-α-actin does not. Instead, in these slightly stretched sarcomeres, the anti–c-α-actin binds the F-α-actin I band complex, leaving the Z-band proper undecorated (inset). The nuclei of the out-of-focus substrate adherent fibroblasts (arrows) tend to be flat ovals. Myotube nuclei tend to be globular. The left asterisk marks an out-of-focus immature myotube juxtaposed to a transfected one. Day 10 MYC/M160-M183–transfected culture, triple stained with (E) anti-MYC, (E′) Rho-phalloidin, and (E′′) DAPI. The asterisks mark an intensely Rho-phalloidin–positive nontransfected immature myotube. Inset reveals that the distribution of Rho-phalloidin along the ~l.0-μm thin filament is more complicated than generally acknowledged in the literature. See Fig. 4. Bar, 10 μm.

myotubes. It was not incorporated selectively into Z-bands in the younger myotubes, but was localized in ectopic fine granules distributed throughout the sarcoplasm and in ectopic longitudinal fibrils/patches (Fig. 5, A–C′′). The MYC/granules are probably self-aggregates since they do not costain with Rho-phalloidin, or with antibodies to any of the I-Z-I proteins tested (see below). Comparable diffuse sarcoplasmic granules positive for endogenous nebulin (e.g., positive for antinebulin NB2) are never observed in nontransfected postmitotic myoblasts or immature or mature myotubes (Lin et al., 1994, 1998; Ojima et al., 1999). The ectopic MYC-positive longitudinal fibrils/patches, which are nested among normal individual SMFs, range in length from 5 to >200 μm, and in width from 0.3 to >5 μm. On the other hand, as shown in Fig. 5 C, most ectopic fibrils/patches costain for both exogenous and endogenous nebulin peptides. Table I summarizes the results of double staining the ectopic fibrils/patches with anti-MYC and antibodies and reagents to other I-Z-I proteins. In contrast to the MYC/granules, most MYC-ectopic fibrils/patches are positive for phalloidin, anti–c-α-actin, antinebulin NB2, and, to a lesser extent, tropomyosin. These ectopic structures are readily distinguished from precursor I-Z-I bodies, for close to 100% of the precursor myofibrillar structures stain discontinuously for titin, s-α-actinin, T-cap, and nebulin (Lin et al., 1998; Ojima et al., 1999). Whether fibrils and patches differ in more subtle details remains to be determined. Of particular interest

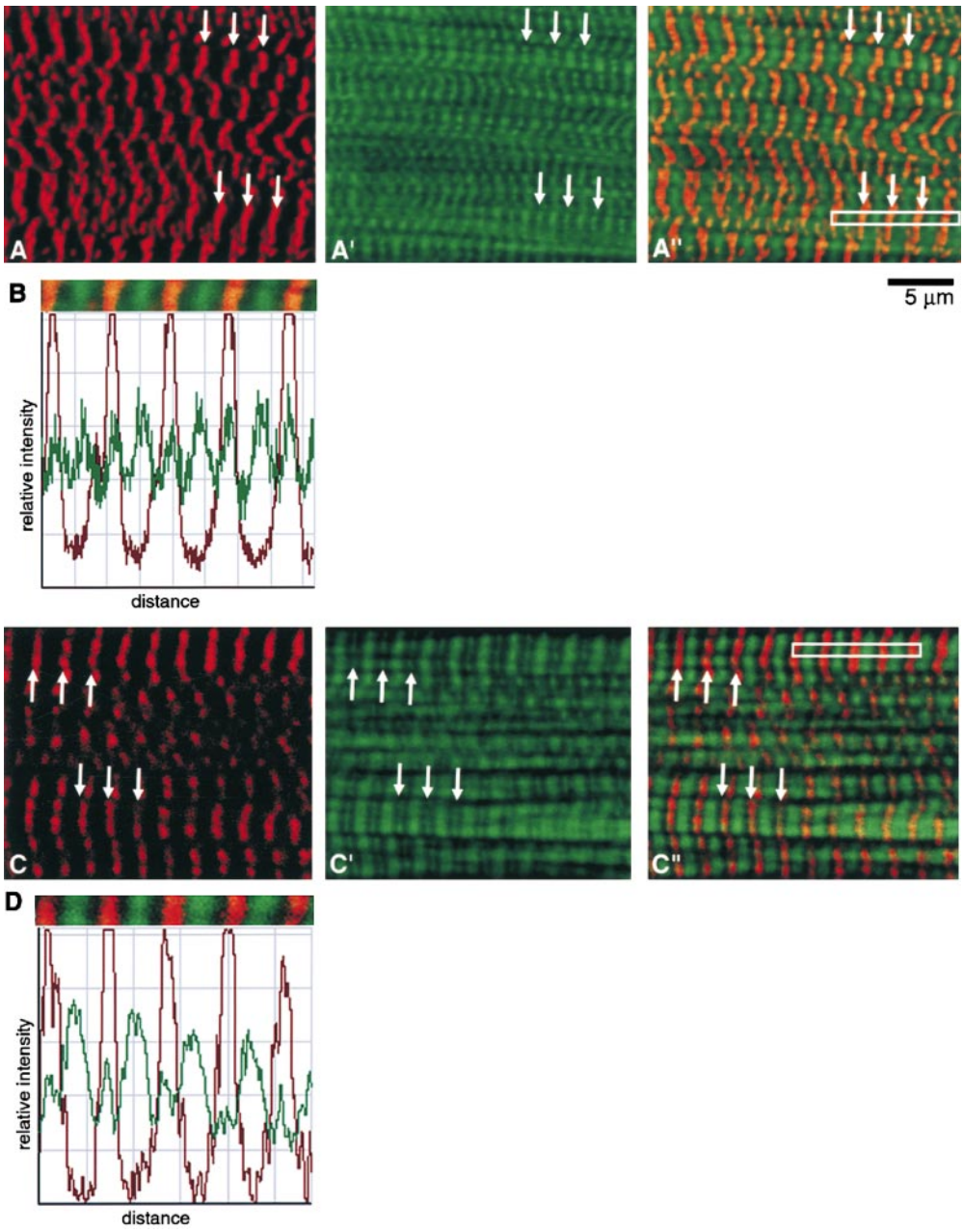

Figure 4. Confocal ~1.0-μm thick sections of mature SMFs from an untransfected (A–A′′) and a transfected (C–C′′) culture similar to that shown in Fig. 3 E. The untransfected myotube was double stained with (A) anti–s-α-actinin and (A′) FITC-phalloidin. A′′ is a merged image of A and A′. The transfected myotube (M160-M183) was double stained with (C) anti-MYC and (C′) FITC-phalloidin. C′′ is a merged image of C and C′. Arrows point to double-stained Z-bands. Owing to the limited resolution of the light microscope, Z-bands that measure ~0.1 μm in the EM, measure 0.20–0.25 μm in the confocal microscope. Further details regarding the variations in width and number of transverse phalloidin-positive bands will be discussed elsewhere. B and D document the relative fluorescence intensity profiles of the five tandem sarcomeres indicated by the white rectangles in Fig. 4, A′′ and C′′, respectively. Bar, 5 μm.

was that between days 4 and 10, there was a progressive diminution in both ectopic MYC/granules and fibrils/patches. Conversely, during this period, MYC/Z-bands became more prominent (Fig. 5, D–D′′). This striking change in localization over time of expressed MYC/M171-M183 was not observed with any of the other MYC/nebulin peptides shown in Fig. 1.

In summary, MYC/M171-M183 was not specifically incorporated into Z-bands in day 4 myotubes, but was incorporated into diffuse granules and fibrils/patches. The loss of these ectopic structures during days 4–6, coupled to the progressive emergence of MYC/Z-bands in day 10 myotubes, suggests the mediation, in older myotubes, of unknown regulatory mechanisms designed to cope with misfolded peptides and/or ectopic structures. Interestingly, Ojima et al. (1999) reported that misoriented ectopic pre-

Table I. Variable Composition of Double-stained MYC/nebulin Ectopic Fibrils/Patches

MYC-positive	Rho-phalloidin–positive	c-α-actin–positive	Nebulin (NB2)-positive	Tropomyosin-positive	S-α-actinin–positive	Titin (Z1Z2)-positive	MHC-positive
100% (n = 210)	93% (n = 30)	67% (n = 30)	60% (n = 30)	37% (n = 30)	3% (n = 30)	0% (n = 30)	0% (n = 30)

Day 10 cultures expressing MYC/M171-M183 were double stained with anti-MYC and Rho-phalloidin, or with antibodies to other myofibrillar proteins. A total of 210 randomly selected MYC-positive fibrils/patches were examined, and the percentage that costained for the other myofibrillar proteins determined.

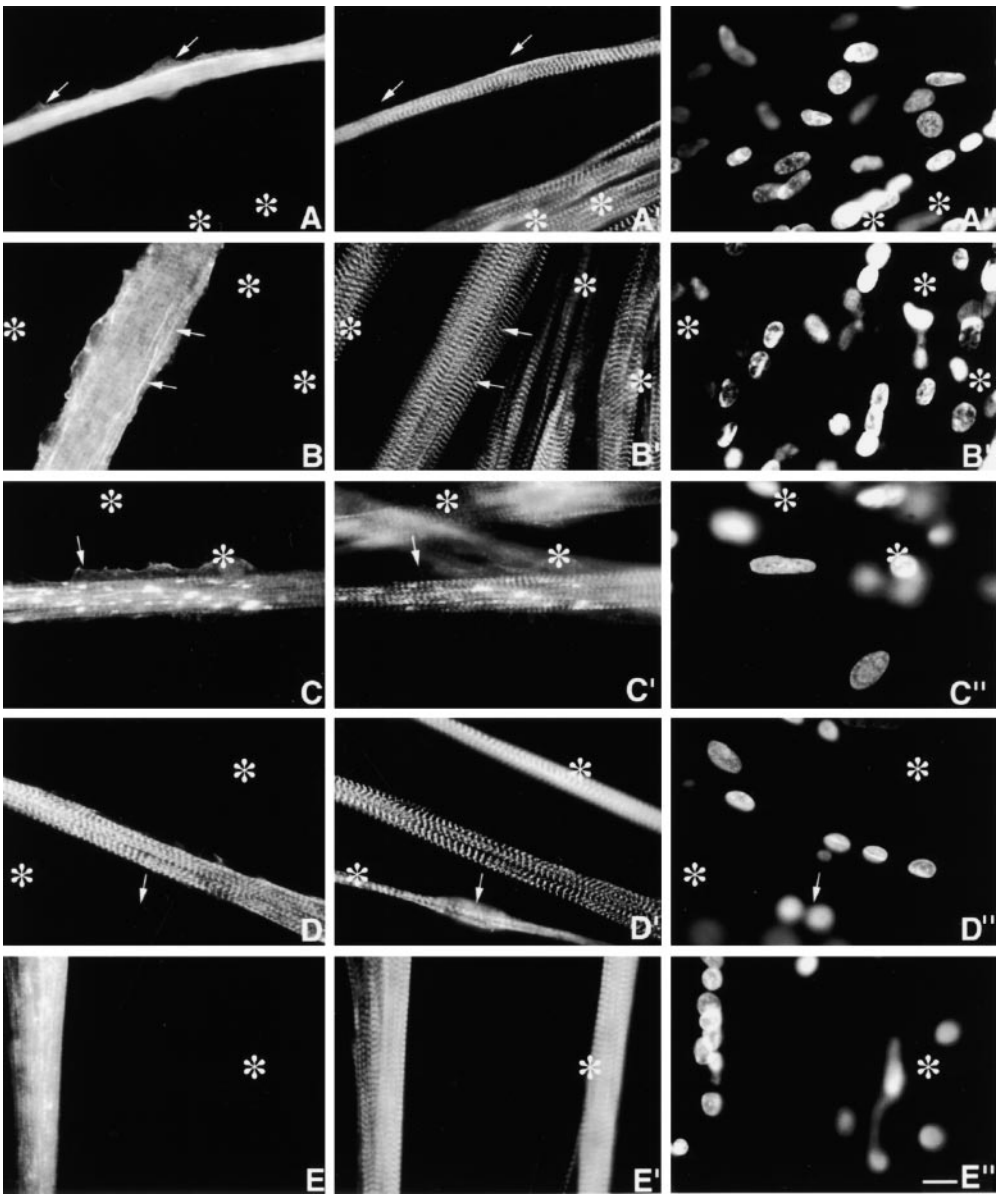

Figure 5. Day 4 MYC/M171-M183–transfected culture, triple stained with (A) anti-MYC, (A′) anti–s-α-actinin, and (A′′) DAPI. Asterisks mark several untransfected myotubes. Fine, diffuse MYC-positive granules are distributed throughout the transfected myotube. Their presence has not detectably interfered with the assembly of morphologically normal periodic Z-bands (A′). Arrows point to lateral sarcoplasmic extensions that are not occupied by SMFs. (B–B′′) Day 6 MYC/M171-M183–transfected culture, triple stained as above. In addition to the ectopic MYC-positive granules, note the ectopic slender nonstriated longitudinal filaments (arrows) that insert between normal SMFs (see below). Neither ectopic MYC-positive structure binds anti–s-α-actinin, nor does it act as a dominant negative. Occasionally, just perceptible MYC/Z-bands can be observed. As discussed in Materials and Methods, these MYC/Z-bands are not likely to be due to bleed-through. Asterisks mark untransfected myotube. Day 6 MYC/M171-M183–transfected culture, triple stained with (C) anti-MYC, (C′) antinebulin (NB2), and (C′′) DAPI. Antinebulin (NB2) localizes to the endogenous nebulin. Note that ~70% of the ectopic MYC-positive filaments/patches costain with antinebulin (NB2). Anti-MYC, but not antinebulin (NB2), accumulates along the edge of the lateral sarcoplasmic extensions (arrows), which lack all myofibrillar structures. MYC/Z-bands are more evident in this day 6 myotube than in younger myotube in Fig. 5 A. Asterisks mark two out-of-focus, overlapping untransfected myotubes. Day 10 MYC/M171-M183–transfected culture, triple stained with (D) anti-MYC, (D′) anti–s-α-actinin, and (D′′) DAPI. Note the elimination of the ectopic MYC-positive granules and filaments/patches in these older myotubes. Asterisks mark out-of-focus untransfected myotubes. Arrow points to an out-of-focus binucleated myotube. Day 4 myotubes expressing MYC/M175-M184. Triple stained with (E) anti-MYC (E′) anti-MHC, and (E′′) DAPI. Ectopic MYC-positive granules and fibrils/patches dominated these transfected cells. MYC-positive Z-bands were not evident. Nevertheless, the morphology of the 1.6-μm A-bands (E′) was normal. Asterisks mark untransfected myotube. Bar, 10 μm.

cursor I-Z-I bodies positive for s-α-actinin, titin, tropomyosin, and troponin were also resorbed in older myotubes.

Localization of MYC/M175-M184

MYC/M175-M184 peptides (Fig. 1) were not incorporated selectively into mature Z-bands at any time. They were primarily incorporated into fine sarcoplasmic granules, fibrils/patches, and occasionally ill-defined striations (Fig. 5, E–E′′). In most respects, they were similar to MYC/M185-Ser (see below). The widespread ectopic MYC-positive structures did not interfere with the assembly of normal SMFs. They did not behave in a dominant negative manner, nor were they obviously cytotoxic, even in day 10 myotubes.

Localization of MYC/M175-SH3

MYC/M175-SH3 (Fig. l) was incorporated into Z-bands in day 4–10-transfected myotubes. Its behavior differed from that of MYC/M160-M183 only in that, occasionally, it was also incorporated into ectopic MYC/fibrils/patches. This

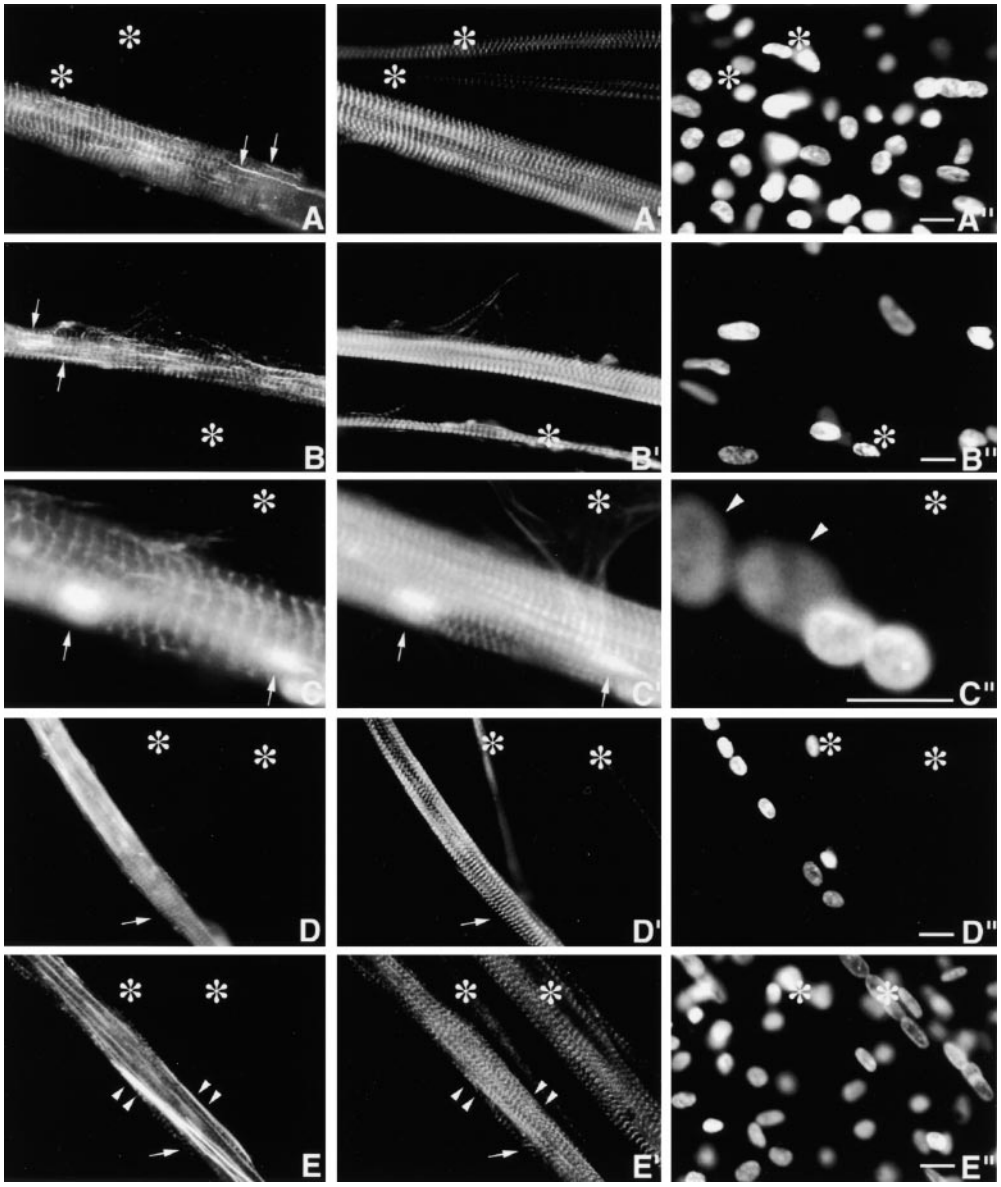

Figure 6. Day 10 myotubes expressing MYC/M175-SH3. Stained with anti-MYC (A, B, and C), anti-titin Z1Z2 (A′), anti-MHC (B′), Rho-phalloidin (C′), and DAPI (A′′, B′′, and C′′). While ectopic fibrils and patches co-stain with anti-MYC and Rho-phalloidin (C, arrows) they do not costain with antibodies to titin Z1Z2 (A′) or MHC (B′). Asterisks in A and B mark untransfected myotube. Asterisks in C, mark out-of-focus Rho-phalloidin–positive fibroblasts. Arrowheads in C′′ mark large nuclei in substrate adherent fibroblasts that lie beneath the myotube, whereas the 2 myotube nuclei are globular. Day 4 MYC/M175-Ser–transfected culture, triple stained with (D) anti-MYC, anti–s-α-actinin (D′), and DAPI (D′′). Transfected myotube exhibits both ectopic MYC-positive fine granules and nonstriated fibrils/patches. Arrow indicates region with just perceptible MYC/Z-bands. Asterisks mark untransfected myotube. (E–E′′) Day 10 MYC/M175-Ser transfected culture, triple stained as in Fig. 6 D. Note the persisting ectopic MYC-positive granules and nonstriated fibrils. Arrows point to faint but morphologically normal MYC-positive Z-bands. Arrowheads mark nonstriated fibrils/patches. Asterisks mark untransfected myotube. Left asterisk marks the growth tip of an immature myotube. Bars, 10 μm.

MYC/peptide was not incorporated into ectopic MYC-positive granules nor into ~1.0-μm F-α-actin thin filament complexes (Fig. 6, A–C′).

Localization of MYC/M175-Ser and MYC/M185-SH3

While being incorporated primarily into diffuse granules and fibrils/patches, both MYC/M175-Ser and MYC/M185-SH3 were also weakly localized in morphologically normal Z-bands (Fig. 6, D–E′′, and Fig. 7, A–A′′). This applied to day 4–10 myotubes. Most frequently, however, the fluorescent intensity of these MYC/Z-bands was modest compared with that of MYC/M160-M183 (Fig. 3, A–E′′) or of MYC/M175-SH3 (Fig. 6, A–C′′). In no instance did either of these MYC/nebulin peptides bind continuously along ~1.0-μm thin filament complexes nor did they behave in a dominant negative fashion.

Localization of MYC/M185-Ser

MYC/M185-Ser peptides were not selectively incorporated into Z-discs in early or late myotubes, but accumulated diffusely throughout the sarcoplasm (Fig. 7, B–C′′). Not infrequently, they displayed a variety of poorly defined cross-banded structures. Their presence did not perceptibly block normal myofibrillogenesis nor were they detectably cytotoxic in myotubes (see below).

Localization MYC/- or GFP/M86-M92

The distribution of MYC/- or GFP/M86-M92 (Fig. 1) also

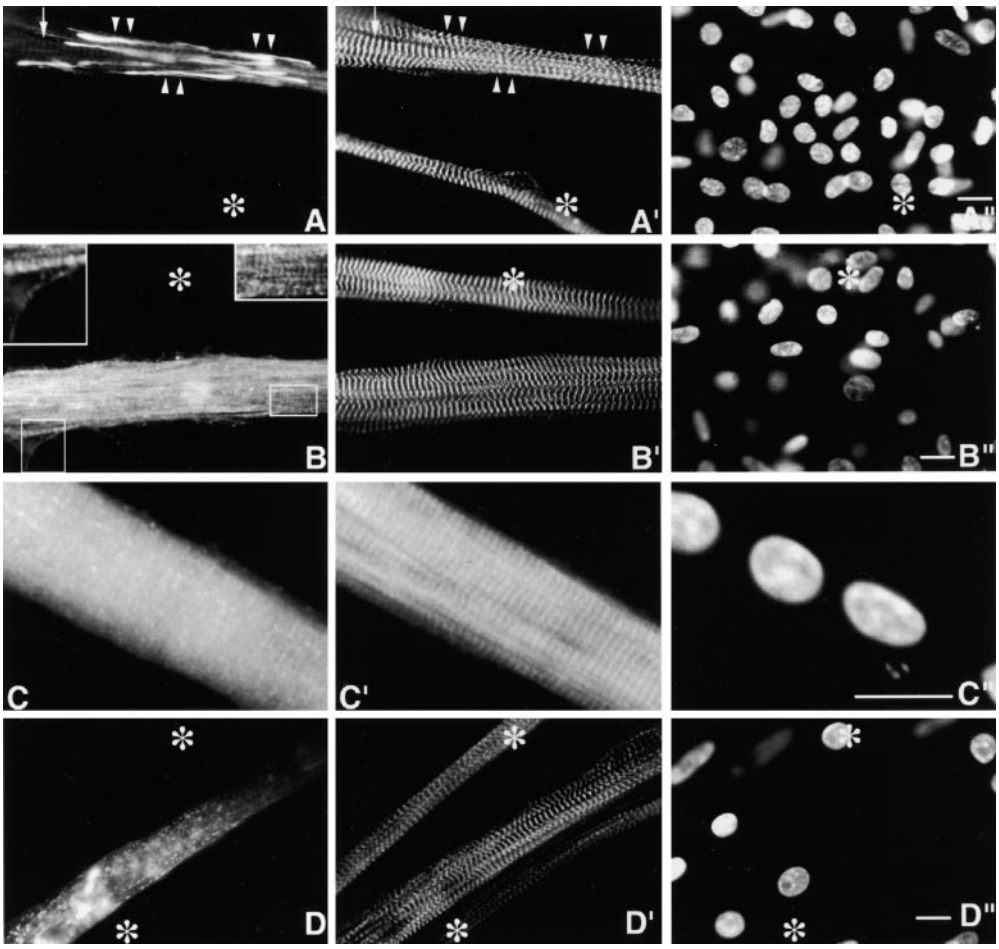

Figure 7. Day 10 MYC/M185-SH3–transfected culture, triple stained with (A) anti-MYC, (A′), anti–s-α-actinin and (A′′) DAPI. Ectopic MYC-positive fibrils/patches (arrowheads) are negative for s-α-actinin. They do not act as dominant negatives. Arrows point to just perceptible normal Z-bands. Day 10 MYC/M185-Ser–transfected culture stained with anti-MYC (B and C), anti–s-α-actinin (B′), Rho-phalloidin (C′), and DAPI (B′′ and C′′). The ill-defined MYC-positive striations shown in B (insets) does not perturb the normal s-α-actinin Z-bands shown in B′. Similarly, the diffuse MYC/granules in C does not alter the multiple Rho-phalloidin cross-bands (C′). Day 10 GFP/M86-M92–transfected myotube viewed in the fluorescein channel (D), in the rhodamine channel (D′) after decoration with rhodamine-labeled anti–s-α-actinin, and in the DAPI (D′′). Similar images were observed in MYC/M86-M92–transfected myotubes (not shown). The GFP-positive fibrils/patches evident in D do not deform the s-α-actinin Z-bands shown in D′. Asterisks mark untransfected myotube in Fig. 7. Bars, 10 μm.

demonstrates that the incorporation of nebulin modules into their site-specific locations in I-Z-I bands requires conditions not yet defined. M86-M92 constitutes the 12th super-repeat of nebulin and in situ is postulated to be located roughly in the middle of ~1.0-μm F-α-actin thin filament complex (Pfuhl et al., 1996). Both the MYC- and the GFP-peptides localized to ectopic granules and fibrils/patches in day 4–10-transfected myotubes (Fig. 7, D and D′). The overall distribution of these tagged fragments was not readily distinguishable from that of COOH-terminal MYC/M175-M184 and MYC/M185-Ser. They were not incorporated into ~1.0-μm thin filament complexes nor were they dominant negatives. The distribution of the 10 tagged nebulin fragments, described in this report, is summarized in Fig. 8.

In Vitro Binding Properties of the Nebulin COOH-terminal SH3 Domain

Recently, high affinity in vitro binding of α-actinin and actin to the SH3 domain of nebulette was described (Moncman and Wang, 1999). On the sequence level, the nebulette and nebulin SH3 domains share 80% sequence identity (Politou et al., 1998), suggesting that the COOH-terminal SH3 domains of nebulin in skeletal muscles and nebulette in heart muscles might be involved in the same protein interactions. To test this, we performed in vitro experiments with nebulin SH3 from human skeletal muscle, and purified F-actin and α-actinin from rabbit muscle. The binding of SH3 to F-actin and α-actinin was studied by sedimenting F-actin in the presence of nebulin SH3 and in the presence of nebulin SH3 together with actin and s-α-actinin. Samples of pellets and supernatants were analyzed on 4–20% SDS gels. When F-actin was sedimented in the presence of nebulin SH3, the nebulin SH3 remained in solution (Fig. 9). This indicates that nebulin SH3 does not bind to F-actin in this cell-free system. To examine whether nebulin SH3 binds to s-α-actinin, a mixture of all three proteins was centrifuged. As seen in Fig. 9, F-actin and α-actinin coprecipitated in a 1:1 ratio, while nebulin was found in the supernatant. Thus, we conclude that the SH3 domain does not bind to actin or α-actinin under the conditions used.

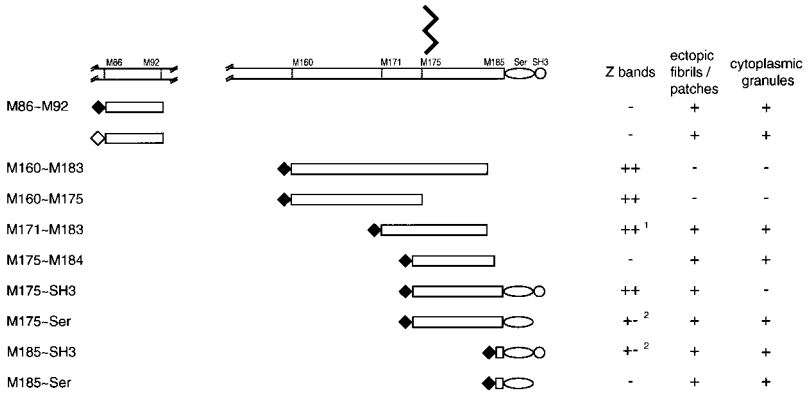

Figure 8. Summary of the respective sites of incorporation of the eight MYC/COOH-terminal peptides and the one peptide, M86-M92, tagged with either MYC or GFP. Unlike those peptides, which were incorporated into Z-bands of day 4 myotubes, M171-M183 was first detected in Z-bands in day 6–10 myotubes. Peptides M175-Ser and M185-SH3 chiefly formed ectopic granules and fibrils/patches, although weakly positive Z-bands could sometimes be observed.

All Nebulin Modules Are Cytotoxic in 72–96-h Posttransfected Mononucleated Cells

Lin et al. (1998) and Ojima et al. (1999) reported that, in myogenic cultures, MYC/s-α-actinin was cytotoxic in most 72–96-h posttransfected mononucleated cells. This applied to both replicating fibroblasts and precursor myogenic cells. In contrast, the same MYC/s-α-actinin fragments were not cytotoxic, even when expressed for as long as 10 d in myotubes. Comparable differences in cytotoxicity between mononucleated cells and myotubes obtain in cultures expressing any of the 10 tagged-nebulin fragments. Roughly 80% of the nebulin-transfected mononucleated cells in day 4 cultures displayed the same moribund cytosyndrome displayed by cells expressing MYC s-α-actinin peptides, namely intensely fluorescent nuclei and cytoplasm, as well as resorption of all cytoskeletal elements including adhesion plaques (Fig. 10, A and B). The frequency of such moribund cells diminished greatly by day 6, and by day 10, was very rare. Hijikata et al. (1997) also reported that MYC/s-α-actinin was cytotoxic in most 72–96-h posttransfected PtK2 cells. Whether the cytotoxic effects of both nebulin and s-α-actinin fragments in mononucleated cells reflects ratios of exogenous peptides/cytoplasmic volume higher in mononucleated cells to that in myotubes, or reflects differences in how myotubes cope with aberrant myofibrillar molecules versus how mononucleated cells cope, requires further experiments.

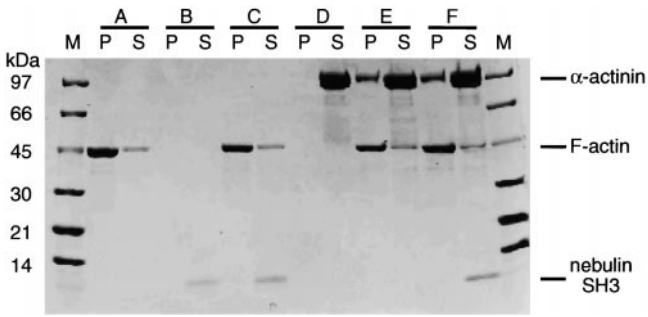

Figure 9. Expressed nebulin SH3 domain does not cosediment in the presence of F-actin and α-actinin. (A) F-α-actin, (B) nebulin SH3, (C) F-α-actin + nebulin SH3, (D) α-actinin, (E) F-α-actin + α-actinin, and (F) F-α-actin + α-actinin + nebulin SH3. P, pellet; S, supernatant; M, molecular marker.

Discussion

The salient observations in this report are as follows. First, there are variations in the capacity of COOH-terminal nebulin modules that incorporated exclusively into Z-bands versus those incorporated ectopically into fine sarcoplasmic granules and fibrils/patches. Second, contrary to the strong binding of nebulin modules to purified F-actin in vitro (Root and Wang, 1994; Pfuhl et al., 1994, 1996; Zhang et al., 1998; Gonsior et al., 1998), the nebulin modules used in this report did not differentially bind to ~1.0-μm F-α-actin thin filament complexes in maturing skeletal myotubes. Third, there are unexpected differences between the visible distribution of F-α-actin in I-Z-I bands after decoration with anti–α-actin versus that after decoration with phalloidin. Fourth, temporospatial differences between sites of incorporation of MYC/M171-M183 in day 4 versus day 10 myotubes (Fig. 5) probably reflect muscle-specific control mechanisms (Wolff et al., 1992; Dhawan et al., 1991) responsible for the turnover of ectopic structures and/or misfolded peptides. Fifth, neither the COOH-terminal Ser nor SH3 domains are obligatory for the incorporation of a subset of nebulin fragments into morphologically normal Z-bands. Finally, MYC/nebulin or GFP/nebulin fragments, which are obviously cytotoxic in day 3–4-mononucleated cells, are not obviously cytotoxic in day 10 maturing myotubes.

Z-bands consisting of α-actin oligomers, s-α-actinin and T-cap molecules, as well as of NH_2-terminal titin and COOH-terminal nebulin residues, have evolved to yield a structure that resists deformation but is essential for force transmission between sarcomeres and for maintaining A-bands in the center of each sarcomere (Horowits, 1999). In such a structure, it might be expected that the stoichiometries and topological interconnections between the proteins would be fixed, rigorously controlled, and that tolerance for the incorporation of misfolded exogenous molecules be minimal. This model of precision crafted, hard-wired interdigitating filaments is consistent with the supposition that both F-α-actin binding proteins, s-α-actinin and nebulin, independently and/or cooperatively, are probably involved in regulating the incorporation and turnover of intra-Z-band F-α-actin. Alternatively, I-Z-I bands may be more compliant and dynamic structures (Schroeter et al., 1996), rich in unsaturated binding sites, designed to exchange ligands rapidly. Glycerinated day

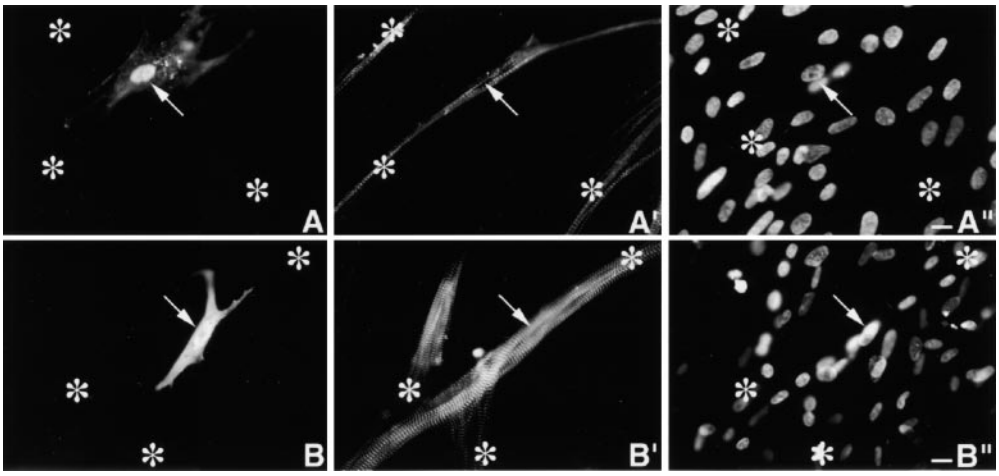

Figure 10. A and B illustrate moribund mononucleated cells in day 3 and day 4 cultures transfected with MYC/M185-Ser. A and B are stained with anti-MYC, A′ and B′ with anti–s-α-actinin, and A′′ and B′′ with DAPI. Arrows point to the intensely fluorescent nuclei in flattened, irregularly shaped moribund mononucleated cells that lie below the immature myotube visualized in A′ and below the more mature myotube visualized in B′. The expressed protein is distributed uniformly throughout the entire cell. Bars, 10 μm.

4–10 myotubes rapidly bind exogenous heavy meromyosin monomers, forming myriad polarized arrowheads uniformly distributed along the entire length of in situ ~1.0-μm F-α-actin thin filament complexes (Ishikawa et al., 1969; Ojima et al., 1999). Similarly, fluorescein-labeled actin, or α-actinin, microinjected into living myogenic cells is promptly incorporated into preexisting I-Z-I structures (Glacy, 1983; McKenna et al., 1985; Sanger et al., 1986). Kunst et al. (2000) reported His6-tagged phosphorylated and unphosphorylated MyBP-C fragments diffused into skinned cardiac myocytes and selectively accumulated in A-bands. Finding that MYC fragments of both s-α-actinin (Schultheiss et al., 1992; Holtzer et al., 1997; Lin et al., 1998; Ojima et al., 1999) and nebulin are incorporated uniquely into Z-bands further supports a model rich in unsaturated binding sites, as well as one unexpectedly tolerant of incorporating some types of aberrant myofibrillar peptides. In developing *Drosophila* muscles, exogenous headless myosin coassembles with endogenous myosin to form thick filaments (Standiford et al., 1997; Cripps et al., 1999). Similarly in dystrophin-deficient *mdx*/ mice truncated utrophin inserts, not just in the sarcolemma subjacent to its normal location in the myoneural junction but displays an ectopic subsarcolemmal global distribution (Tinsley et al., 1996), and dystrophin fragments can be incorporated into a morphologically normal sarcolemma and mediate the assembly of the dystrophin-associated glycoprotein complex (Lu et al., 2000). Whether SMFs with MYC/Z-bands function properly or in myotubes older than day 10 would prove to be a dominant negative and induce nemaline-like bodies (e.g., Schultheiss et al., 1992; Lin et al., 1998) or be cytotoxic, must still be determined.

Assuming that nebulin modules 177–185 plus the Ser and SH3 domains are integral to Z-bands, whereas the more NH_2-terminal modules are integrated uniformly into the polarized ~1.0-μm thin filaments, then normally only 5–7% of the length of nebulin is confined to the Z-lattice. It will be interesting to determine whether the four MYC/COOH-terminal fragments that are incorporated exclusively into Z-bands in myotubes will bind to F-actin, as well as to other integral Z-band peptides in cell free systems and whether any modules NH_2-terminal to M160-M175 are incorporated selectively into Z-bands. Alternatively, the intracellular integration into Z-bands of a subset of COOH-terminal nebulin peptides may require the concurrent and cooperative interactions of several Z-band components, or even of assemblases (Barral and Epstein, 1999), as has been postulated for the integration of s-α-actinin fragments into Z-bands (Ojima et al., 1999).

Our findings do not exclude the possibility of favorable electrostatic conditions that permit side-by-side binding of positively charged nebulin modules to the negatively charged surface of intra-Z-band F-α-actin oligomers (Amann et al., 1998), or the grove near the phalloidin binding site at the center of the actin α-helix. Zhang et al. (1998) and Gonsior et al. (1998) reported that despite their insolubility, some nebulin modules could be incorporated into F-actin and cosediment in a cell-free system. Microscopically, such in vitro reconstituted F-actin/nebulin aggregates resemble the ectopic fibrils/patches assembled in myotubes (Fig. 5, B and C, Fig. 6, A and E, and Fig. 7 A). Recently, comparable findings have been observed with different titin N2A fragments. Ojima, K., Z. Lim, and H. Holtzer (unpublished data) found that the incorporation of titin GFP/I80-I81 was tightly regulated because it incorporated exclusively at the same level in the I-bands as that occupied by the equivalent residues of the in situ wild-type titin. In contrast, titin GFP/I76-I79 and GFP/PEVK were distributed diffusely throughout the entire sarcoplasm. Whether the spatially appropriate incorporation of fragments of nebulin or titin into SMFs involves a novel type of dimerization with their respective in situ full-length amino acid residues must be investigated. This type of modular exchange might be limited to the turnover of exceptionally long proteins with reiterative receptors.

The presence of homologous SH3 and Ser domains in the COOH termini of both nebulin and nebulette has prompted speculations regarding their role in the assembly of I-Z-I bands (Millevoi et al., 1998; Politou et al., 1998; Young et al., 1998; Moncman and Wang, 1999). However, as summarized in Fig. 8, M160-M183 and M160-M175, which lack both SH3 and Ser domains have the capacity to be incorporated into Z-bands. Thus far, we have

not identified any single site that is obligatory for the incorporation of nebulin fragments into Z-bands.

Recently, Moncman and Wang (1999) studied the effects of expressing nebulette modules in cultured-mononucleated cardiomyocytes. While some of our findings are in agreement with some of their conclusions, many are not. Several reasons could account for these differences. First, the method of isolating the SH3 domains differed in the two studies (see Materials and Methods). Second, there was ambiguity regarding the sites of incorporation of the expressed nebulette in the cardiac I-Z-I bands, based on phalloidin to identify actin; and third, despite the sequence similarities of the COOH-terminal nebulin and nebulette, the functions of these regions in the assembly and maintenance of the I-Z-I bands in the two phenotypes may be less conserved. In our opinion, however, the most likely explanation derives from a common misunderstanding of the behavior of the already differentiated cardiomyocytes in culture versus the behavior of presumptive skeletal myoblasts and their daughter myoblasts in culture.

Cardiomyocyte cultures are seeded with fully differentiated cells taken from the developing chick. 100% of such cardiomyocytes have already assembled thousands of contracting mature SMFs before being cultured. In contrast, skeletal myogenic cultures are seeded with mononucleated cells, none of which has assembled any myofibrillar structures. In day 4–10 cardiomyocyte cultures >90% of the SMFs previously assembled in ovo are in various stages of degeneration: only a minute fraction of the myofibrillar structures in these cells is in some stage of assembly (Dlugosz et al., 1984; Lin et al., 1989; Handel et al., 1991; Lu et al., 1992). In contrast, >98% of the myotubes in day 4–10 cultures of skeletal myogenic cells are rich in thousands of de novo assembled stable, invariant, mature SMFs (Holtzer et al., 1972, 1997; Lin et al., 1987, 1998; Fig. 2). The extent of massive degeneration of the preformed SMFs in cultures of differentiated cardiomyocytes has been grossly underestimated in the literature (e.g., Lin et al., 1989; Schultheiss et al., 1990; Lu et al., 1992; Messerli et al., 1993; Simpson et al., 1996; Sussman et al., 1997; Linke et al., 1999). In brief, the global degeneration, attributed by Moncman and Wang (1999) to the dominant negative effects of exogenous nebulette may rather be the result of the spontaneous fragmentation of SMFs, which is characteristic of both untransfected and transfected cultured cardiomyocytes (e.g., compare the virtual identity of micrographs in the untransfected cardiomyocytes in Lin et al. (1989) with the transfected cardiomyocytes in Moncman and Wang, 1999). Much is yet to be learned of both the similarities, but particularly of the differences, between myofibrillogenesis in cardiac versus skeletal muscle.

The emergence of MYC/Z-bands in day 10 MYC/M171-M183 myotubes, which is correlated with the progressive loss of ectopic MYC structures in day 4–6 myotubes (Fig. 5, A–D), suggests selective turnover and/or posttranslational changes that would be missed in the absence of time-dependent studies. The simplest explanation is that, despite their impaired conformation, the increased concentration reaches a critical level over time, which permits these particular modules to out compete wild-type ligands for incorporation into morphologically normal Z-bands; alternatively, the ectopic MYC/M171-M183 structures were selectively degraded. Precedent for the selective elimination of ectopic myofibrillar structures has been described recently. Misaligned I-Z-I bodies, which consist of linear aggregates of s-α-actinin/nebulin/titin/α-actin/T-cap, are resorbed within 24–48 h in the giant growth tips of elongating myotubes (details in Ojima et al., 1999). Despite differences in morphologies and molecular composition, the selective resorption of ectopic MYC/s-α-actinin I-Z-I bodies, and MYC/nebulin granules or fibrils/patches, might involve similar surveillance systems. Until more is known about the kinetics of the turnover of full-length nebulin in living myotubes, as well as of those of the other integral Z-band proteins, speculations about how nebulin modules might be integrated into, or excluded from, normal Z-band structures, or how they are resorbed from ectopic structures, are premature. By following the fate of GFP/nebulin modules over time (e.g., 4–30 d; Holtzer et al., 1972) in living myotubes, we should be able to determine the following: whether their incorporation is regulated by the same mechanisms that control normal turnover; whether the exogenous modules fully displace the wild-type nebulin over time, or only their COOH termini, and whether such incorporation feeds back on the regulation of either the translation or transcription of the gene for endogenous nebulin.

We thank Dr. Z.Q. Zhang (Beijing Medical School) for helpful technical support. We are indebted to Dr. John Murray (University of Pennsylvania) for many helpful suggestions.

This work was supported by grants 5-P01-HL15835 and Hl59470 from the National Institutes of Health and from the Muscular Dystrophy Association.

Submitted: 18 April 2000
Revised: 12 June 2000
Accepted: 12 June 2000

References

Amann, K.J., B.A. Renley, and J.M. Ervasti. 1998. A cluster of basic repeats in the dystrophin rod domain binds F-actin through an electrostatic interaction. *J. Biol. Chem.* 273:28419–28423.

Antin, P.B., S. Tokunaka, V.T. Nachmias, and H. Holtzer. 1986. Role of stress fiber-like structures in assembling nascent myofibrils in myosheets recovering from exposure to ethyl methanesulfonate. *J. Cell Biol.* 102:1464–1479.

Ao, X., and S.S. Lehrer. 1995. Phalloidin unzips nebulin from thin filaments in skeletal myofibrils. *J. Cell Sci.* 108:3397–3403.

Barral, J.M., and H.F. Epstein. 1999. Protein machines and self assembly in muscle organization. *Bioessays.* 21:813–823.

Bukatina, A., B. Sonkin, L. Alievskaya, and V. Yashin. 1984. Sarcomere structures in the rabbit psoas muscle as revealed by fluorescent analogs of phalloidin. *Histochemistry.* 81:301–304.

Bullard, B., J. Bell, R. Craig, and K. Leonard. 1985. Anthrin: a new actin-like protein in insect flight muscle. *J. Mol. Biol.* 182:443–454.

Cripps, R.M., J.A. Suggs, and S.I. Bernstein. 1999. Assembly of thick filaments and myofibrils occurs in the absence of the myosin head. *EMBO (Eur. Mol. Biol. Organ.) J.* 18:1793–1804.

Dhawan, J., L.C. Pan, G.K. Pavlath, M.A. Travis, A.M. Lanctot, and H.M. Blau. 1991. Systemic delivery of human growth hormone by injection of genetically engineered myoblasts. *Science.* 254:1509–1512.

Dlugosz, A.A., P.B. Antin, V.T. Nachmias, and H. Holtzer. 1984. The relationship between stress fiber-like structures and nascent myofibrils in cultured cardiac myocytes. *J. Cell Biol.* 99:2268–2278.

Franke, W.W., S. Stehr, S. Stumpp, C. Kuhn, H. Heid, H.-R. Rackwitz, M. Schnölzer, R. Baumann, H.-J. Holzhausen, and R. Moll. 1996. Specific immunohistochemical detection of cardiac/fetal α-actin in human cardiomyocytes and regenerating skeletal muscle cells. *Differentiation.* 60:245–250.

Gautel, M., A. Mues, and P. Young. 1999. Control of sarcomeric assembly: the flow of information on titin. *Rev. Physiol. Biochem. Pharmacol.* 138:97–137.

Glacy, S.D. 1983. Pattern and time course of rhodamine-actin incorporation in cardiac myocytes. *J. Cell Biol.* 96:1164–1167.

Goldstein, M.A., J.P. Schroeter, and L.H. Michael. 1991. Role of the Z band in the mechanical properties of the heart. *FASEB (Fed. Am. Soc. Exp. Biol.) J.* 5:2167–2174.

Gonsior, S.M., M. Gautel, and H. Hinssen. 1998. A six-module human nebulin fragment bundles actin filaments and induces actin polymerization. *J. Muscle Res. Cell Motil.* 19:225–235.

Gregorio, C.C., K. Trombitas, T. Center, B. Kolmerer, G. Stier, K. Kunke, K. Suzuki, F. Obermayr, B. Herrmann, H. Granzier, H. Sorimachi, and S. Labeit. 1998. The NH_2-terminal of titin spans the Z-disc: its interaction with a novel 19-kD ligand (T-cap) is required for sarcomeric integrity. *J. Cell Biol.* 143:1013–1027.

Gregorio, C.C., H. Granzier, H. Sorimachi, and S. Labeit. 1999. Muscle assembly: a titianic achievement? *Curr. Opin. Cell Biol.* 11:15–25.

Handel, S., M. Greaser, E. Schultz, S. Wang, J. Bulinski, J. Lin, and J. Lessard. 1991. Chicken cardiac myofibrillogenesis with antibodies specific for titin and the muscle and non-muscle isoforms of actin and tropomyosin. *Cell Tissue Res.* 263:419–430.

Hijikata, T., Z. Lin, S. Holtzer, J. Choi, H.L. Sweeney, and H. Holtzer. 1997. Unanticipated temporal and spatial effects of sarcomeric α-actinin peptides expressed in PtK2 cells. *Cell Motil. Cytoskel.* 38:54–74.

Holtzer, H., J. Sanger, H. Ishikawa, and K. Strahs. 1972. Selected topics in myofibrillogenesis. *Cold Spring Harbor Symp. Quant. Biol.* 37:549–566.

Holtzer, H., T. Hijikata, Z.X. Lin, Z.Q. Zhang, S. Holtzer, F. Protasi, C. Franzini-Armstrong, and H.L. Sweeney. 1997. Independent assembly of 1.6 μm long bipolar MHC filaments and I-Z-I bodies. *Cell Struc. Funct.* 22:83–93.

Horowits, R. 1999. The physiological role of titin in striated muscle. *Rev. Physiol. Biochem. Pharmacol.* 138:57–96.

Ishikawa, H., R. Bischoff, and H. Holtzer. 1969. Formation of arrowhead complexes with heavy meromyosin in a variety of cell types. *J. Cell Biol.* 43:312–328.

Kruger, M., J. Wright, and K. Wang. 1991. Nebulin as a length regulator of thin filaments of vertebrate skeletal muscles: correlation of thin filament length, nebulin size, and epitope profile. *J. Cell Biol.* 115:97–107.

Kunst, G., K. Kress, M. Gruen, M. Gautel, and R. Fink. 2000. Myosin binding protein C, a phosphorylating-dependent force regulator in muscle that controls the attachment of myosin heads by its interaction with myosin S2. *Circ. Res.* 86:51–58.

Labeit, S., and B. Kolmerer. 1995. The complete primary structure of human nebulin and its correlation to muscle structure. *J. Mol. Biol.* 248:308–315.

Labeit, S., T. Gibson, A. Lakey, K. Leonard, M. Zeviani, P. Knight, J. Wardale, and J. Trinick. 1991. Evidence that nebulin is a protein-ruler in muscle thin filaments. *FEBS (Fed. Eur. Biochem. Soc.) Lett.* 282:313–316.

Langer, B., and F. Pepe. 1980. New rapid method for purifying α-actinin from chicken gizzard and skeletal chicken pectoral muscle. *J. Biol. Chem.* 255: 5429–5434.

Lin, Z., J.R. Eshelman, S. Forry-Schaudies, S. Duran, J.L. Lessard, and H. Holtzer. 1987. Sequential disassembly of myofibrils induced by phorbol myristate acetate in cultured myotubes. *J. Cell Biol.* 105:1365–1376.

Lin, Z., S. Holtzer, T. Schultheiss, J. Murray, T. Masaki, D. Fischman, and H. Holtzer. 1989. Polygons and adhesion plaques and the disassembly and assembly of myofibrils in cardiac myocytes. *J. Cell Biol.* 108:2355–2367.

Lin, Z., M.H. Lu, T. Schultheiss, J. Choi, S. Holtzer, C. DiLullo, D.A. Fischman, and H. Holtzer. 1994. Sequential appearance of muscle-specific proteins in myoblasts as a function of time after cell division: evidence for a conserved myoblast differentiation program in skeletal muscle. *Cell Motil. Cytoskel.* 29:1–19.

Lin, Z., T. Hijikata, Z. Zhang, J. Choi, S. Holtzer, H.L. Sweeney, and H. Holtzer. 1998. Dispensability of the actin-binding site and spectrin repeats for targeting sarcomeric α-actinin into maturing Z bands in vivo: implications for in vitro binding studies. *Dev. Biol.* 199:291–308.

Linke, W., D. Rudy, T. Centner, M. Gautel, C. Witt, S. Labeit, and C. Gregorio. 1999. I-band titin in cardiac muscle is a three-element molecular spring and is critical for maintaining thin filament structure. *J. Cell Biol.* 146:631–644.

Lu, M.H., C. DiLullo, T. Schultheiss, S. Holtzer, J.M. Murray, J. Choi, D.A. Fischman, and H. Holtzer. 1992. The vinculin/sarcomeric-alpha-actinin/alpha-actin nexus in cultured cardiac myocytes. *J. Cell Biol.* 117:1007–1022.

Lu, Q., G. Morris, S. Wilson, T. Ly, P. Strong, and T. Partridge. 2000. Massive idiosyncratic exon skipping corrects the nonsense mutation in dystrophic mouse muscle and produces functional revertant fibers by clonal expansion. *J. Cell Biol.* 148:985–995.

Maruyama, K. 1997. Connectin/titin, giant elastic protein of muscle. *FASEB (Fed. Am. Soc. Exp. Biol.) J.* 11:341–345.

Messerli, J., M. Eppenberger, P. Schwab von Arx, and J.-C. Perriard. 1993. Remodeling of cardiomyocyte cytoarchitecture visualized by three dimensional confocal microscopy. *Histochemistry.* 100:193–202.

McGough, A., B. Pope, W. Chiu, and A. Weeds. 1997. Cofilin changes the twist of F-actin: implications for actin filament dynamics and cellular function. *J. Cell Biol.* 138:771–781.

McKenna, N.M., J.B. Meigs, and Y.L. Wang. 1985. Exchangeability of α-actinin in living cardiac fibroblasts and muscle cells. *J. Cell Biol.* 101:2223–2232.

Miller, J.B., S.B. Teal, and F.E. Stockdale. 1989. Evolutionarily conserved sequences of striated muscle myosin heavy chain isoforms. Epitope mapping by cDNA expression. *J. Biol. Chem.* 264:13122–13130.

Millevoi, S., K. Trombitas, B. Kolmerer, S. Kostin, J. Schaper, K. Pelin, H. Granzier, and S. Labeit. 1998. Characterization of nebulette and nebulin and emerging concepts of their roles for vertebrate Z-discs. *J. Mol. Biol.* 282: 111–123.

Moncman, C.L., and K. Wang. 1999. Functional dissection of nebulette demonstrates actin binding of nebulin-like repeats and Z-line targeting of SH3 and linker domains. *Cell Motil. Cytoskel.* 44:1–22.

Morris, E.P., G. Nneji, and J.M. Squire. 1990. The three-dimensional structure of the nemaline rod Z-band. *J. Cell Biol.* 111:2961–2978.

Mues, A., P.F. van der Ven, P. Young, D.O. Fürst, and M. Gautel. 1998. Two immunoglobulin-like domains of the Z-disc portion of titin interact in a conformation-independent way with telethonin. *FEBS (Fed. Exp. Biochem. Soc.) Lett.* 428:111–114.

Nagaoka, R., K. Kusano, H. Abe, and T. Obinata. 1995. Effects of cofilin on actin filamentous structures in cultured muscle cells. *J. Cell Sci.* 108:581–593.

Ojima, K., Z.X. Lin, Z.Q. Zhang, T. Hijikata, S. Holtzer, S. Labeit, H.L. Sweeney, and H. Holtzer. 1999. Initiation and maturation of I-Z-I bodies in the growth tips of transfected myotubes. *J. Cell Sci.* 112:4101–4112.

Otey, C.A., M.H. Kalnoski, and J.C. Bulinski. 1988. Immunolocalization of muscle and nonmuscle isoforms of actin in myogenic cells and adult skeletal muscle. *Cell Motil. Cytoskel.* 9:337–348.

Pfuhl, M., S.J. Winder, and A. Pastore. 1994. Nebulin, a helical actin binding protein. *EMBO (Eur. Mol. Biol. Organ.) J.* 13:1782–1789.

Pfuhl, M., S.J. Winder, M.A.C. Morelli, S. Labeit, and A. Pastore. 1996. Correlation between conformational and binding properties of nebulin repeats. *J. Mol. Biol.* 257:367–384.

Politou, A.S., S. Millevoi, M. Gautel, B. Kolmerer, and A. Pastore. 1998. SH3 in muscles: solution structure of the SH3 domain from nebulin. *J. Mol. Biol.* 276:189–202.

Root, D.D., and K. Wang. 1994. Calmodulin-sensitive interaction of human nebulin fragments with actin and myosin. *Biochemistry.* 33:12581–12591.

Sanger, J.M., B. Mittal, M.B. Pochapin, and J.W. Sanger. 1986. Myofibrillogenesis in living cells microinjected with fluorescently labeled α-actinin. *J. Cell Biol.* 102:2053–2066.

Schroeter, J.P., J.P. Bretaudiere, R.L. Sass, and M.A. Goldstein. 1996. Three-dimensional structure of the Z band in a normal mammalian skeletal muscle. *J. Cell Biol.* 133:571–583.

Schultheiss, T., Z.X. Lin, M.H. Lu, J. Murray, D.A. Fischman, K. Weber, T. Masaki, M. Imamura, and H. Holtzer. 1990. Differential distribution of subsets of myofibrillar proteins in cardiac nonstriated and striated myofibrils. *J. Cell Biol.* 110:1159–1172.

Schultheiss, T., J. Choi, Z.X. Lin, C. DiLullo, L. Cohen-Gould, D. Fischman, and H. Holtzer. 1992. A sarcomeric α-actinin truncated at the carboxyl end induces the breakdown of stress fibers in PtK2 cells and the formation of nemaline-like bodies and breakdown of myofibrils in myotubes. *Proc. Natl. Acad. Sci. USA.* 89:9282–9286.

Simpson, D., W. Sharp, T. Borg, R. Price, L. Terracio, and A. Samarel. 1996. Mechanical regulation of cardiac myocyte protein turnover and myofibrillar structure. *Am. J. Physiol.* 270:C1075–C1087.

Standiford, D.M., M.B. Davis, K. Miedema, C. Franzini-Armstrong, and C.P. Emerson Jr. 1997. Myosin rod protein: a novel thick filament component of *Drosophila* muscle. *J. Mol. Biol.* 265:40–55.

Studier, F., A. Rosenberg, J. Dunn, and J. Dubendroff. 1990. Use of T7 RNA-polymerase to direct expression of cloned genes. *Methods Enzymol.* 185: 60–89.

Sussman, M., S. Hamm-Alvarez, P. Vialta, P. Welch, and L. Kedes. 1997. Involvement of phosphorylation in doxorubicin-mediated myofibril degeneration: an immunofluorescence microscopy analysis. *Circ. Res.* 80:52–61.

Takekura, H., H. Shuman, and C. Franzini-Armstrong. 1993. Differentiation of membrane systems during development of slow and fast skeletal muscle fibres in chicken. *J. Muscle Res. Cell Motil.* 14:633–645.

Tinsley, J.M., A.C. Potter, S.R. Phelps, R. Fischer, J.I. Trickett, and K.E. Davies. 1996. Amelioration of the dystrophic phenotype of *mdx* mice using a truncated utrophin transgene. *Nature.* 384:349–353.

Toyama, Y., S. Forry-Schaudies, B. Hoffman, and H. Holtzer. 1982. Effects of taxol and colcemid on myofibrillogenesis. *Proc. Natl. Acad. Sci. USA.* 79: 6556–6560.

van Straaten, M., D. Goulding, B. Kolmerer, S. Labiet, J. Clayton, and B. Bullard. 1998. Association of kettin with actin in the Z-disc of insect flight muscle. *J. Mol. Biol.* 285:1549–1562.

Vigoreaux, J.O. 1994. The muscle Z band: lesson in stress management. *J. Muscle Res. Cell Motil.* 15:237–255.

Wang, K., and C.L. Williamson. 1980. Identification of an N2 line protein of striated muscle. *Proc. Natl. Acad. Sci. USA.* 77:3254–3258.

Wang, K., and J. Wright. 1988. Architecture of the sarcomere matrix of skeletal muscle: immunoelectron microscopic evidence that suggests a set of parallel inextensible nebulin filaments anchored at the Z line. *J. Cell Biol.* 107:2199–2212.

Wang, K., M. Knipfer, Q.-Q. Huang, A. van Heerden, L.C. Hsu, G. Gutierrez, X.-L. Quian, and H. Stedman. 1996. Human skeletal muscle nebulin sequence encodes a blueprint for thin filament architecture. *J. Biol. Chem.* 271: 4304–4314.

Wilson, P., E. Fuller, and A. Forer. 1986. Irradiation of rabbit myofibrils with an ultraviolet microbeam. II. Phalloidin protects actin in solution but not in myofibrils from depolymerization by ultraviolet light. *Biochem. Cell Biol.* 65: 376–385.

Wolff, J.A., J.J. Ludtke, G. Acsadi, P. Williams, and A. Jani. 1992. Long-term persistence of plasmid DNA and foreign gene expression in mouse muscle. *Hum. Mol. Genet.* 1:363–369.

Wright, J., Q. Huang, and K. Wang. 1993. Nebulin is a full length template of actin filaments in the skeletal muscle sarcomere: an immunoelectron micro-

scopic study of its orientation and span with site specific monoclonal antibodies. *J. Muscle Res. Cell Motil.* 14:476–483.

Yamaguchi, M., M. Izumimoto, R.M. Robson, and M.H. Stromer. 1985. Fine structure of wide and narrow vertebrate muscle Z-lines. A proposed model and computer simulation of Z-line architecture. *J. Mol. Biol.* 184:621–643.

Yasuda, K., T. Anazawa, and S. Ishiwata. 1995. Microscopic analysis of the elastic properties of nebulin in skeletal myofibrils. *Biophys. J.* 68:598–608.

Young, P., C. Ferguson, S. Banuelos, and M. Gautel. 1998. Molecular structure of titin of the sarcomeric Z-disc: two types of titin interactions lead to an asymmetrical sorting of alpha-actinin. *EMBO (Eur. Mol. Biol. Organ.) J.* 17: 1614–1624.

Zhang, J.Q., A. Weisberg, and R. Horowits. 1998. Expression and purification of large nebulin fragments and their interaction with actin. *Biophys. J.* 74: 349–359.

Zhukarev, V., J.M. Sanger, J.W. Sanger, Y.E. Goldman, and H. Shuman. 1997. Distribution and orientation of rhodamine-phalloidin bound to thin filaments in skeletal and cardiac myofibrils. *Cell Motil. Cytoskel.* 37:363–377.